IEEE Access
Multidisciplinary | Rapid Review | Open Access Journal

Received 16 June 2022, accepted 16 July 2022, date of publication 19 July 2022, date of current version 26 July 2022.

*Digital Object Identifier 10.1109/ACCESS.2022.3192415*

RESEARCH ARTICLE

# A Semi-Supervised Modulation Identification in MIMO Systems: A Deep Learning Strategy

**SOFYA BOUCHENAK[1], RACHID MERZOUGUI[1,2], FOUZI HARROU[3], (Senior Member, IEEE), ABDELKADER DAIRI[4,5], AND YING SUN[3]**

[1]STIC Laboratory, Faculty of Engineering Science of Tlemcen, Tlemcen 13000, Algeria
[2]EASPM Laboratory, Faculty of Engineering of Saida, Saïda 20000, Algeria
[3]Computer, Electrical and Mathematical Sciences and Engineering (CEMSE) Division, King Abdullah University of Science and Technology (KAUST), Thuwal 23955-6900, Saudi Arabia
[4]Université des Sciences et de la Technologie d'Oran Mohamed-Boudiaf (USTOMB), Oran 31000, Algeria
[5]Laboratoire des Technologies de l'Environnement (LTE), Ecole Nationale Polytechnique, Oran 31000, Algeria

Corresponding author: Fouzi Harrou (fouzi.harrou@kaust.edu.sa)

This work was supported by the King Abdullah University of Science and Technology (KAUST), Office of Sponsored Research (OSR), under Award OSR-2019-CRG7-3800.

**ABSTRACT** Accurate modulation identification of the received signals is undoubtedly a central component in multiple-input multiple-output (MIMO) communication systems, facilitating the demodulation task. This study presents a flexible and semi-supervised deep learning-driven strategy for automatic modulation identification. To this end, the multiclass classification problem is treated as multiple binary discrimination problems to address modulation identification challenges. Here, we merge the features extraction ability of the Generative Adversarial Network (GAN) model and the semi-supervised anomaly detection scheme, the one-class Support Vector Machine (1SVM). Essentially, a single GAN-based 1SVM detector is trained using training data of each class, with the samples of that class as inlier and all other samples as anomalies (i.e., one-vs.-rest). The 1SVM is trained using the features learned by the GAN model. A dataset consisting of three digital modulations (i.e., BFSK, CPFSK, and PAM4) and three analog modulations (i.e., AM-DSB, AM-SSB, and WB-FM), widely used in wireless communications systems, is employed to demonstrate the performance of the considered deep learning-based methods. Compared to Restricted Boltzmann Machine (RBM) and Deep Belief Network (DBN)-based 1SVM, the conventional GAN, DBN, and RBM with softmax layer as discriminator layer, the proposed GAN-based 1SVM detector offers superior discrimination performance of modulation types by achieving an averaged accuracy of 0.951 and F1-Score of 0.954. Results also showed that the GAN-1SVM detector dominates the state-of-the-art modulation classification techniques.

**INDEX TERMS** Modulation recognition, MIMO systems, deep learning, GAN, semi-supervised anomaly detection.

## I. INTRODUCTION

Communication systems are experiencing tremendous growth and fast development in today's competitive atmosphere due to the massive need for information dissemination. With higher expectations for meeting the increased requirement in terms of speed and underlying diversity to support the increased capacity of different systems, spatial multiplexing techniques, such as multiple-input and multiple-output (MIMO) and massive MIMO, is becoming a critical component in the recent generation of communication network systems [1]. Several signals in space come from different systems with distinct modulation types on different frequencies are received, and it is essential to recognize and monitor them for numerous military and civilian applications [2]. Discriminating signals from different systems makes modulation and demodulation techniques crucial elements for ensuring wireless data transmission [3], [4]. Importantly, the modulation classification (MC) consists in automatically discovering the modulation type of the received signals

The associate editor coordinating the review of this manuscript and approving it for publication was Wei Wei.


This work is licensed under a Creative Commons Attribution 4.0 License. For more information, see https://creativecommons.org/licenses/by/4.0/

with limited or without prior information on the signals parameters [5].

Crucially, modulation enables a certain level of encryption, particularly in the military domain, making difficult the message decryption at the reception without knowing the type of modulation used on transmission [6], [7]. Thus, the modulation types must be reliably identified in noncooperative communication systems to guarantee reliable data transmission. To this end, discriminating modulation types is undoubtedly a pivotal element to carefully address for achieving correct demodulation [8], [9]. Of course, developing effective and automatic modulation classification techniques is essential to maintain high transmission quality, and it is a non-trivial task from both communication researchers and engineers [10]. In recent years, modulation detection techniques have become necessary for military and commercial applications, e.g., in coding transmission and spectrum management. Various procedures aimed at identifying modulation types have been reported in the litterature [7], [10], [11]. For instance, in [12], an approach based on Independent Component Analysis (ICA) has been applied to classify different modulation types in A MIMO system. The challenge in classifying modulation in MIMO systems involves handling a set of different signals at the receiving antenna array. However, in this approach, noise variance is assumed to be known. In [13], the authors introduced a blind modulation classification approach for a MIMO system without knowing channel matrix and noise variance. At first, an Expectation-Maximization (EM) algorithm is applied for every modulation candidate to estimate the channel parameters. Here, the obtained estimation is utilized for the likelihood assessment of the corresponding modulation candidate. Then, the maximum likelihood criterion is used in the classification decision. Results indicate satisfactory classification for BPSK, QPSK, and 16-QAM modulations under white Gaussian noise conditions. In [14], authors addressed modulation classification as a clustering problem for every modulation type. Then, the maximum likelihood criteria are applied for the final classification decision. Results show that this modulation classifier has a robust performance for a low SNR. The authors in [5] introduced an approach for modulation classification for PSK signals based on random graphs. Essentially, this approach is designed through the graph's connectivity formed using the Fourier transform of the second and fourth powers of the acquired signal. Experiments are conducted using PSK signals generated by Rohde&Schwarz generator and analyzer. It has been shown that this approach can be used to classify phase-shift keying (PSK) signals in MIMO systems. In [15], a modulation classifier has been presented for multipath signals based on cepstrum. At first, this approach eliminates the impact of multipath channel coefficient using the cepstrum-based preprocessing technique and then applies a logarithmic functional fitting approach for modulated signals classification. Experimental results reveal this approach's capacity in discriminating quadrature PSK (QPSK), 16-ary quadrature amplitude modulation (16QAM), and 4QAM. In [16], a coupled approach is introduced to classify modulation of MIMO-OFDM signals by combing ICA and support vector machines (SVM). At first, the ICA JADE technique is performed for separating the data streams of the MIMO-OFDM signal. After that, maximum likelihood and SVM are applied to detect the modulation of separate data streams. This approach achieved 85% classification rates for SNR high than 15 dB.

Accurately recognizing modulation type is increasingly important in wireless communications for enhancing radio performance. The main objective of this paper is to design a deep learning-driven detector for modulation identification in MIMO systems, which is an essential component in numerous communications systems. As a data-driven, the introduced modulation discrimination approach could be used for both SISO and MIMO systems under varying channel conditions, such as multipath fading, which is not the case of many procedures in the literature. Moreover, this approach is performed without estimating channel/signal-to-noise ratio (SNR) nor timing and frequency offset correction. In addition, this is a semi-supervised approach that does not require labeled data to construct a model to discriminate different types of modulation from the received signal in MIMO systems. Unlike supervised approaches, semi-supervised methods are more attractive for modulation discrimination since it is not always easy to get accurately labeled data. Of course, the paper has the following contributions

- This study presents a semi-supervised deep hybrid model for modulation identification in MIMO systems. To this end, the multiclass classification problem is treated as multiple binary discrimination problems. Specifically, we merge the features extraction ability of the Generative Adversarial Network GAN) model and the detection sensitivity of the one-class Support Vector Machine algorithm (1SVM). This choice is motivated by the flexibility of the GAN model in learning relevant information from complex data without the need for labeled data or prior hypotheses on data distribution. In addition, 1SVM is an efficient anomaly detection scheme due to its capability for learning linear and nonlinear decision boundaries to detect anomalies. As we know, this is the first time that this hybrid deep learning model has been applied for automatic modulation discrimination. Indeed, first, for each modulation, we construct a single GAN-based 1SVM detector using training data of the considered class, with the samples of that class as inlier and all other samples as anomalies (i.e., one-vs.-rest). Then, each detector is used to sense a specific modulation from the received signals. This approach builds up a detector to distinguish between modulation types. The extracted features from the received signals using the trained GAN discriminator are used as the input of the 1SVM scheme. The core concept of 1SVM consists of determining a hyper-plan closer to the training data samples corresponding to a

specific modulation, and no labeling is needed to construct 1SVM. After that, the newly received samples are classified as comparable or distinct from the training data. Of course, 1SVM is a semi-supervised binary classifier that has been widely exploited for anomaly detection in different applications.

- Furthermore, for comparison purposes, we investigated other deep learning models for modulation identification, including Deep Belief Network (DBN) and restricted Boltzmann machine (RBM)-based 1SVM methods, as well as the GAN, DBN, and RBM with softmax layer as discriminator layer for multi-classes classification. As far as we know, this is the first time that these methods have not been explored before for modulation classification. The publically available RadioML 2016.10A dataset is employed in this study to assess the efficiency of investigated deep learning-based methods. Five statistical indices are employed to compare the discrimination accuracy of the considered methods: accuracy, precision, recall, F1Score, and the Area Under the Curve (AUC). Results demonstrate the effectiveness of the proposed GAN-1SVM detector for automatic modulation identification and its superior performance compared to the other models and the state-of-the-art techniques.
- Finally, we compared the discrimination performance of the GAN-1SVM detector with the state-of-the-art methods, and showed the capacity of the proposed approach to improve automatic modulation identification.

The rest of the paper is structured as follows. Section II presents the related work. Section III presents the preliminary material required in the proposed modulation detection approach given Section IV. Section V conducts the experiments to assess the proposed approach and compare it with the baselines. Finally, concluding remarks and some future lines of improvement are provided in Section VI.

## II. RELATED WORK

Recently, deep learning has emerged as a promising research line to improve the performance of communication technologies, both in academia and in industry [17]–[19]. Essentially, deep learning methods are an efficient tool for automatically retrieving pertinent information from high-dimensional and voluminous datasets without the need for manual features [20]. Deep learning techniques have been applied for different application, such as communication technologies [21], resource allocations [22], traffic control [23] and modulation classification [17]. Nevertheless, deep learning technologies have not been well exploited and explored in communications systems. Until recently, few studies have focused on exploring deep learning technologies for modulation classification, a crucial element in non-cooperation communications. For instance, in [24], a two steps-based deep learning approach called cascaded convolutional neural network (CasCNN) has been introduced to classify PSK and QAM modulation formats. This approach is formed of a two-block of CNN. The first block is employed to classify the modulation type, while the second one is used to identify the indexes of the modulations. An accuracy of 90% is obtained by using CasCNN at SNR of 4 dB and the symbol length of 256. The authors in [19] employed the CNN and the long short-term memory (LSTM) for modulation classification. The advantage of the CNN-LSTM model is its ability to effectively exploring feature correlation and the spatial-temporal characteristics of raw complex temporal signals; the spatial features are extracted using CNN, while LSTM is powerful in learning time-dependent in time series data. Here, two streams interact in pairs are used to learn the features; one stream (i.e., CNN-LSTM) extracts the local raw temporal features from raw signals, and the other stream (i.e., CNN-LSTM) learns the knowledge from amplitude and phase information. Results indicate that the CNN-LSTM improved modulation classification compared with some existing state-of-the-art methods. In [17], a Gated Recurrent Unit (GRU)-based deep learning approach is proposed for modulation classification with resource-constrained end-devices. The classification is performed using a SoftMax layer as an output of the GRU model. It has been shown that the GRU-driven model reaches a classification accuracy of 92.4% with a memory footprint of 73.5 kBytes (51.74% less than the base approach). The study in [18] investigates the application feasibility of two deep learning models, AlexNet and GoogLeNet, for modulation classification using signal constellation diagrams. To this end, different data conversion techniques have generated gray images, enhanced gray images, and three-channel images. Results showed the superior performance of deep learning models for modulation classification compared to traditional methods. In [25], a deep learning network with three hidden layers is used for modulation classification using 21 features, including cumulants and instantaneous amplitude. The network has been randomly initialized rather than using the greedy layer-wise algorithm for pretraining, making it difficult to exploit the full capacity of deep learning. In [26], ResNet deep neural-driven approach, primarily constructed for images classification, is applied to identify modulation formats. However, its performance is limited because the time-series data is different from spatially distributed images.

Bahloul *et al.* considered two higher-order cumulants of the transmitted signal streams for classifying modulation types in MIMO systems [27]. They introduced a soft-decision fusion technique to find the classification result. In [28], a classifier based on random graph theory is employed to identify M-Quadrature Amplitude Modulation (QAM) signals for MIMO Systems under unsatisfactory channel conditions. In this approach, the features obtained using discrete Fourier transform and sparse transform are used by the undirected random graph for classifying the M-QAM signals. This approach showed satisfactory classification results based on simulated data. In [29], a three-dimensional convolutional network-based approach has been proposed to classify MIMO-OFDM modulation from received signals. This

approach learns the modulation patterns based on the assumption of unknown frequency-selective fading channels and SNR. Simulation results showed that this approach reaches the classification accuracy of around 95% at 0 dB SNR. In [30], Wang *et al.* considered a supervised deep learning framework to automatically classify modulation in MIMO systems using the convolutional neural network-based zero-forcing (CNN-ZF) approach. Simulation results revealed that the CNN-ZF approach achieved better classification performance than the artificial neural network with high order cumulants when applied under the perfect channel state information condition. However, results showed that the performance of the CNN-ZF method is influenced not only by the channel's error coefficient but also by the number of antennas at the transmission (Nt) and the reception (Nr). For instance, simulated results showed that the CNN-ZF approach achieved high classification performance when the channel error coefficient equals 0.2 and SNR=10db, Nr=4, and Nt=1. Nevertheless, the performance of this approach has been significantly degraded by obtaining an accuracy of 50% when using four receiving antennas and four transmitting antennas. The study in [31] focused on the problem of classification of Superimposed Modulations for 5G MIMO two-way cognitive relay network over Nakagami-m channels by using a MultiBoosting (MultiBoostAB) classifier. Simulation results showed satisfactory classification performance of the MultiBoostAB classifier even at low SNR. Also, it has been shown that this approach exhibited superior performance compared to the J48 classifier. Gao *et al.* proposed Distribution Test Ensemble (DTE) classifier to classify M-QAM and M-PSK modulations in MIMO systems [32]. They included weather data such as cloud cover and temperature as predictors. They achieved better classification accuracy than other distribution test classifiers in different channel conditions. They also showed that even the DET is inferior to the machine learning classifier in the AWGN channel, the DTE provides reasonable modulation classification with lower computational complexity than machine learning classifiers. Wang *et al.* introduced a cooperative approach based on a convolutional neural network (CNN) to recognize the modulation types in MIMO systems [33]. To this end, at first, CNN obtained the classification sub-results from every received antenna in the MIMO systems. After that, a final decision is accomplished using the sub-results and cooperative decision rules. Simulation results indicated the promising performance of the coupled CNN and weighty averaging decision rule in classifying modulation types. Zhang *et al.* presented a generalized CNN-driven technique for modulation recognition in IoT systems [34]. This approach has been constructed using data with varying noise conditions, making it more robust compared to the conventional CNN approach. Results show the superior classification capacity of this approach compared to the conventional CNN. Much research has been done on designing modulation identification mechanisms for MIMO systems. For example, see some relevant review papers [9], [35]–[37].

## III. METHODOLOGY

This section briefly introduces the modulation recognition problem, the GAN models, and the 1SVM-based detector used to develop our GAN-based 1SVM modulation identification approach.

### A. MODULATION RECOGNITION PROBLEM

This section aims to provide a basic idea behind the modulation classification problem. Generally speaking, the main elements in wireless communication systems with modulation classification components consist of a transmitter and a channel model at the system level. The simplified schematic presentation of a wireless communication system with a modulation classification unit is depicted in Figure 1. Essentially, the modulation recognition component is an intermediate procedure between signal detection and demodulation on the receiver side. The modulation recognition task aims to identify the modulation type of the received signal to facilitate understanding the type of communications system and emitter present. For more details about communication system components see [38], [39].

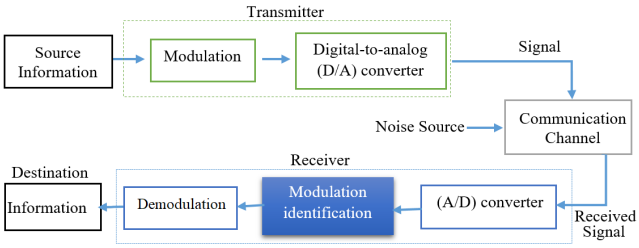


**FIGURE 1.** A simple illustration of a signal model processing framework.

The received data on the receiver side is a contaminated version of the emitted data because of different channel impairments and noise measurements. Thus, the received data $r_t$ can formulated as,

$$y_t = x_t * c_t + n_t, \tag{1}$$

where $x_t$ denotes the modulated signal, $c_t$ refers to the impulse response of the transmitted wireless channel, and $n_t$ represents is the additive noise. On the transmitter side, the central role of the modulator is to map the information signal (also called modulating signal), $v(t)$, into one of the carrier parameters. The resulting signal from the modulator is the modulated signal, $x_t$, which is expressed as:

$$x(t) = \Re(v(t)A_c exp(j2\pi f_c t)) \tag{2}$$

$$= A_c a(t) cos(2\pi f_c t + \phi(t)), \tag{3}$$

$Ac$ and $fc$ refer to the carrier magnitude and the carrier frequency of the carrier signal, respectively.

At the receiver side, the demodulation task intends to strip the information signal from the carrier. This could be correctly accomplished after recognizing the type of modulation used in the received signal. The most simple receiver to recognize an unknown modulation scheme employed a brute-force

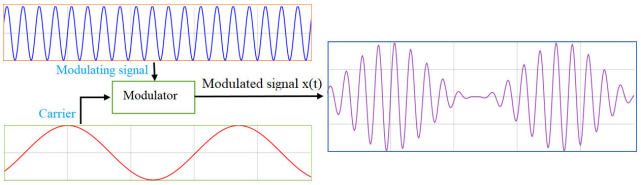


**FIGURE 2.** Illustrative example of a modulation procedure.

search strategy by applying several demodulators for every specific modulation type. By using this strategy, only the demodulator corresponding to the correct modulation can achieve the desired performance. However, the implementation of this strategy is computational and time-consuming, which makes it undesirable solution. As an alternative, a more proficient and attractive strategy for modulation recognition is based on analyzing the received data using data-driven methods, particularly the machine learning paradigm.

Classically, modulation recognition is treated in supervised modulation classification as a multiclass classification problem. More specifically, each class corresponds to a specific modulation; we have $N$ classes classification problem for $N$ modulation types. Crucially, the central objective of modulation recognition consists in maximizing the value of

$$P_i = P(x_t \in N_i | y_t), \tag{4}$$

based on the received signal $y(t)$, where $N_i$ denote the ith category of all the modulation types.

### B. GENERATIVE ADVERSARIAL NETWORKS

GANs have recently emerged as effective and efficient deep learning models for data generation and learning data representations from unlabeled data [40]–[42]. GAN has been successfully applied in various areas, such as image data generation and learning, time-series prediction [43]. Conventionally, GANs contain two neural networks called a generator $\mathcal{G}$ and a discriminator $\mathcal{D}$, which are placed in an adversarial way. They are trained in unsupervised way, making them very attractive as labeling is an expensive task. Moreover, the GAN's generator and discriminator could be trained via only backpropagation. GAN adopts a clever procedure in training: the generator model is trained to continually generate fake data, while the discriminator model seeks to identify between true and fake (generated) data. Traditionally, the Generator model is trained to capture the distribution of the training data and generate new data. At the same time, the discriminator is simultaneously trained to discriminate real from generated samples(Figure 3). An adversarial competition process trains the two networks to improve the quality of the generated data, which becomes progressively comparable to the ground truth (training data). The GAN is optimized once the Nash equilibrium between the two models is obtained, i.e., superior discriminative ability and suitability generate the fake data with approximatively identical distribution to the ground truth [44].

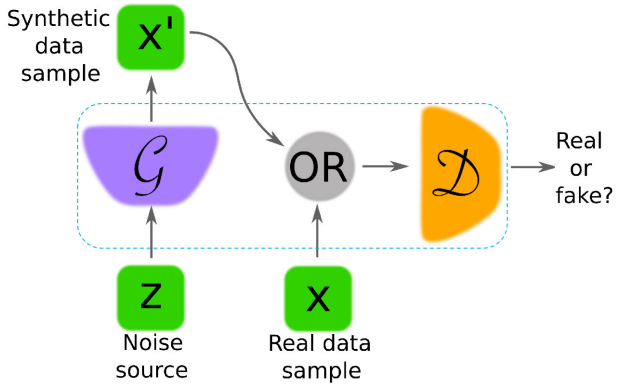


**FIGURE 3.** GAN architecture.

Given noise data $z$ distributed following the distribution $p_z(z)$ (usually uniform distribution), the generator generated data with distribution $p_g(x)$. Then, together with the generated and the ground truth data $p_{data}(x)$, are sent to the discriminator, which tries to discriminate the original data from the generated one. As a composite model, the GAN consists of two-loss functions, the generator and discriminator losses. Minimizing the GAN loss function ( known as the min-max loss) is performed by maximizing $\mathcal{D}(x)$ and minimizing $\mathcal{D}(\mathcal{G}(z))$. The GAN training aims to solve the following optimization problem [45]:

$$\min_G \max_D \mathcal{V}(\mathcal{G}, \mathcal{D}) = \mathbb{E}_{x\sim p_{data}}[log\mathcal{D}(x)] + \mathbb{E}_{z\sim p_z}[log(1-\mathcal{D}(\mathcal{G}(z)))] \tag{5}$$

The parameters of the discriminator are updated in training via the stochastic gradient given in (6).

$$\nabla_{\theta d} \frac{1}{m} \sum_{i=1}^{m} [log(\mathcal{D}(x^i)) + log(1-\mathcal{D}(G(z^i)))]. \tag{6}$$

While the generator updates the model parameter via a descending stochastic gradient (7).

$$\nabla_{\theta g} \frac{1}{m} \sum_{i=1}^{m} log(1-\mathcal{D}(G(z^i))). \tag{7}$$

The discriminator D function convergence is given in (8).

$$\mathcal{D}^* = \frac{P_data(x)}{P_data(x) + P_g(z)}, \tag{8}$$

where $P_data(x)$ refers to the training data distribution and $P_g(z)$ is the learned distribution. See [45] for further details about the GAN model. Crucially, the GAN model is constructed by alternately updating the generator's parameters and a discriminator using the batch (a subset sampled from the training data). Even if GAN was initially designed for computer vision problems, the adversarial training procedure attained promising performance for the prediction problems.

Of course, the GAN model is trained via a self-supervised procedure by alternately optimizing the generative and discriminative networks to learn representations of unlabelled

data [45]. The goal of the training step is to learn the true distribution that generates the data to resemble the received signals. Once the model is trained, the discriminator network is employed for the rest of the study as the role of the generator is to support the discriminator in differentiating true from fake (noisy) data. The discriminator automatically extracts the effective features that provide a compact continuous representation of the received signals. In this study, the extractor features from the trained GAN model will be used as input for 1SVM to discriminate the types of modulation used in the received signals. Thus, the next section is dedicated to the description of the 1SVM approach.

### C. ONE CLASS SVM

This section expounds on the idea of a one-class SVM (1SVM) algorithm adopted in this study for modulation identification. The 1SVM algorithm is one of the most popular anomaly detection techniques, known for its insensitivity to noise measurements and outliers in training. Crucially, the 1SVM is based on two essential concepts, maximizing the margin and mapping the data to a high dimensional feature space induced by a kernel function [46]. It should be noted that 1SVM is a semi-supervised binary classifier [47], [48]. More specifically, the 1SVM is constructed using unlabeled training data that contains inliers samples (anomaly-free data). In the training stage, the 1SVM process consists of estimating a boundary area, which contains most of the training data. This is carried out by determining a hyperplane with the largest distance to the nearest training data [49]. After that, the designed 1SVM is used to identify anomalies (outliers) by checking if a new test data falls within this boundary or not. Of course, testing data points are declared normal (inlier) if they are within the previously defined boundary; otherwise, they are identified as an anomaly (outliers). The 1SVM procedure assures finding a hyperplane that produces a good data separation by using kernel tricks. Figure 4 provides a basic illustration of the 1SVM-based anomaly detection concept.

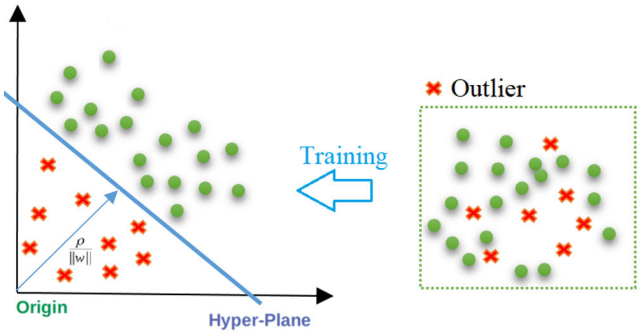


**FIGURE 4.** A basic illustration of 1SVM procedure.

Of course, 1SVM aims to classify one class of data and separate it from any other possible samples (Figure 4). The samples from the normal class can be classified as inlier by the 1SVM; however, any distinct data compared to the normal data will be classified as outliers. In other words, the 1SVM is trained to reject data that are dissimilar from the training data. As a semi-supervised anomaly detection approach, 1SVM has gained attention in different applications, such as photovoltaic plant supervision [50], uncovering obstacles in self-driving cars [51], detection of abnormal air pollution [52], and water quality monitoring [53].

The essence anomaly detection using the 1SVM scheme is first trained the 1SVM to recognize normal behavior and then used to decide on whether the tested data is normal or not (outliers). To this end, samples are mapped in high-dimensional space to facilitate separating samples by using kernel tricks. Explicitly, 1SVM separates the data by determining the hyper-plan that optimizes the data-origin separation margin. This optimization problem is given as:

$$\min_{\omega\gamma\rho}\left(\frac{1}{2}\omega^T\omega-\rho+\frac{1}{\upsilon l}\sum_{i=1}^{l}\gamma_i\right)$$
$$\text{Subject to}: \ \omega.\,\Psi(x)>\rho-\gamma \tag{9}$$

where $l$ denotes the training data size, $\omega$ refers to a weight vector, $\upsilon \in (0,1]$ represents the regularization factor, whereas $\gamma$ refers to the non-zero slack variable employed to penalize the samples that do not lie within the decision boundary in the training phase. Furthermore, $\rho$ is the margin separating the origin from the mapped samples in feature space, known as offset. The 1SVM applies a decision function $\mathcal{F}$ defined in (10) that provides $-1$ for an outlier and 1 for a typical sample using the predefined hyper-plane.

$$\mathcal{F}(x)=sign\left(\omega.\,\Psi(x)-\rho\right) \tag{10}$$

Here, $\Psi$ denotes a nonlinear function (i.e., kernel) employed to project data into feature space. The term $\frac{\rho}{\|\omega\|}$ denotes the hyper-plane (Figure 4), and it is, indeed, the Euclidean distance separating the origin from the support vector points; this term needs to be maximized. Support vector points refer to the points closer to the hyperplane and affect the orientation and position of the hyperplane. The 1SVM quadratic optimization problem is presented in (11).

$$\min_{\omega\gamma\rho}\left(\frac{\|\omega\|^2}{2}-\rho+\frac{1}{\upsilon l}\sum_{i=1}^{l}\gamma_i\right). \tag{11}$$

Thus, in the 1SVM training process, the aim is to maximize the margin $\frac{\|\omega\|^2}{2}-\rho$ and minimizes the average of the slack variables $\gamma$. In this work, the Gaussian radial base function (RBF) $\mathcal{K}$ (12), a popular kernel used for 1SVM due to its flexibility, is utilized.

$$\mathcal{K}(x,x')=\langle\Psi(x),\Psi(x')\rangle=e^{(\alpha\|x-x'\|^2)} \tag{12}$$

where $\alpha$ refers to a parameter controlling how dissimilar $x$ is to $x'$.

Since the 1SVM is built using unlabeled data, it is well suited for modulation identification in MIMO systems. In addition, the 1SVM detector is known to be robust to noise

in the training data. Leveraging on the desirable properties of the GAN methodology and 1SVM detector, this paper aims to develop a semi-supervised approach to discriminate between different types of modulations based on the received signals.

## IV. THE PROPOSED FRAMEWORK

This study introduces a proficient and semi-supervised approach to automatically identify modulation types in MIMO systems. Specifically, this approach is the coupled GAN-1SVM detector, which addresses modulation classification as an anomaly detection problem. The general framework of the proposed modulation identification approach is presented in Figure 5.

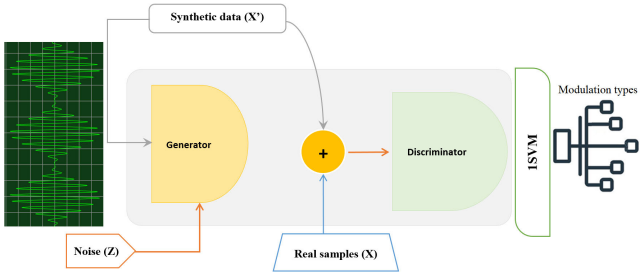


**FIGURE 5.** Illustration of the modulation identification framework.

The core idea in this work is to construct a GAN-based deep learning model for each modulation type. Feature extraction is crucial to the success of modulation identification. Essentially, the GAN learns the distribution of the underlining training data. The learning procedure comprises two phases. Firstly, the Generator and Discriminator are trained in a competitive way to learn the distribution of the training data to generate a real-like distribution. The parameters of the discriminator model are fine-tuned to reach the global optimum. Moreover, in the GAN-1SVM approach, the output of the GAN model is used to feed the 1SVM scheme. In training, the 1SVM maps the GAN features into kernel space and determines the threshold hyper-plan that separates the data points (inliers) from the origin. Crucially, the GAN-1SVM is constructed to recognize each class separately without any data labeling, which makes it very attractive for online applications.

An innovative modulation identification technique based on deep learning and the semi-supervised once-class SVM is introduced in this study (Figure 6). In short, the GAN model is employed as a feature extractor to learn relevant information from the received signal, and the 1SVM checks the output of the GAN discriminator to identify the modulation type. Figure 6 summarizes the main steps in the proposed GAN-driven 1SVM modulation recognition. In the preprocessing stage, the training data is normalized via min-max normalization within the interval [0, 1] and used for model training.

The normalization of the received signals, $\mathbf{y}$, is accomplished using the following formula.

$$\widetilde{y} = \frac{(y - y_{min})}{(y_{max} - y_{min})}, \tag{13}$$

where $y_{min}$ and $y_{max}$ refer to the minimum and maximum of the raw received signals, respectively.

For each modulation type, we first train the 1SVM utilizing the GAN discriminator output based on training data that contains only data for a specific modulation (Figure 6). Note that unlabeled data is used for 1SVM construction. The training phase's essence consists of determining a hyper-plan as close as possible to the normal samples (data from a specific modulation type). Unlike supervised methods, 1SVM as a semi-supervised method needs only the data of normal samples (i.e., signals related to a specific modulation) in training and without labeling. After that, the constructed GAN-1SVM is applied to evaluate the dissimilarity of the new test samples from the training samples. Note that it is not always easy to get accurately labeled data of different modulation types in MIMO systems, making the semi-supervised GAN-1SVM approach very appealing in practice.

In this study, five statistical scores commonly used in the literature are employed to quantify the performance of the studied methods computed using a $2 \times 2$ confusion matrix (Table 1): Accuracy, Precision, Recall, F1-Score, and Area under curve (AUC). For a binary detection task, the number of true positives (TP), false positives (FP), false negatives (FN), and true negatives (TN) are employed to compute the evaluation metrics from a $2 \times 2$ confusion matrix. The accuracy (14) calculates the fraction of data points that are correctly recognized. Recall (15) refers to the capacity to recognize modulation type correctly. Precision (16) point out the success probability of correctly identifying modulation type. The F1-score (17) calculates the harmonic average of precision and recall. These evaluation metrics have values in the range [0, 1], where 1 means the highest performance.

**TABLE 1.** A 2 × 2 confusion matrix.

| | | Identified modulation | |
|---|---|---|---|
| | | Positive | Negative |
| Actual Modulation | Positive | True Positive (TP) | False Negative (FN) |
| | Negative | False Positive (FP) | True Negative (TN) |

$$\text{Accuracy} = \frac{\text{TP} + \text{TN}}{\text{TP} + \text{FP} + \text{TN} + \text{FN}}. \tag{14}$$

$$\text{Recall} = \frac{\text{TP}}{\text{TP} + \text{FN}}. \tag{15}$$

$$\text{Precision} = \frac{\text{TP}}{\text{TP} + \text{FP}}. \tag{16}$$

$$\text{F1} - \text{Score} = 2\frac{\text{Precision.Recall}}{\text{Precision} + \text{Recall}} = \frac{2\text{TP}}{2\text{TP} + \text{FP} + \text{FN}}. \tag{17}$$

## V. RESULTS AND DISCUSSION

### A. DATA DESCRIPTION

The efficiency of the proposed method is verified using the public datasets RadioML.2016.10a, which is widely used as a benchmark in modulation recognition [54]. In addition, this

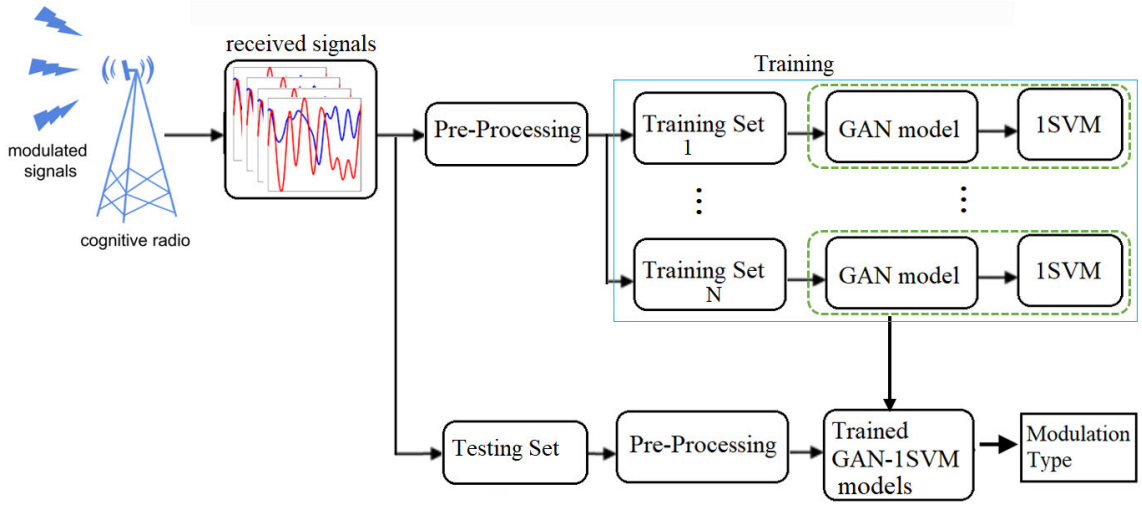


**FIGURE 6.** Illustration of the GAN-based 1SVM modulation identification framework.

dataset comprises modulations that are widely used in wireless communications systems globally. More specifically, this data comprises radio signals synthetically simulated via the GNU Radio. More specifically, this data contains radio signals with different modulations (three analog modulation and eight digital modulations) collected under varying SNR levels from $-20$ dB to $+18$ dB with a step of 2 dB. Generally, signals transmitted via radio channels are tainted with different effects. The generated data have been passed via several channel imperfections and intersymbol interference to mimic the realistic wireless systems. Specifically, the RadioML.2016.10a data are generated by considering these non-ideal effects, including thermal noise, symbol timing offset, Doppler, and phase difference [55]. This study assessed the considered modulation identification approaches using a dataset consisting of six modulations. We considered three digital modulations, Binary Phase Shift Keying (BPSK), Continuous-phase Frequency-shift Keying (CPFSK), and Pulse Amplitude Modulation 4 (PAM4) and three analog modulations (i.e., Amplitude Modulation-Single Side-band Modulation(AM-SSB), AM-Double Side-band (AM-DSB), and Wide-band Frequency Modulation (WBFM)), widely used in wireless communications systems. The datasets have been modulated by a rate of eight samples per symbol using a normalized average transmit power of 0 dB.

Figure 7 provides an example of the time evolution of the raw complex signal at the receiver for different considered modulation types. We observe that the received signals are tainted with noise measurements because of channel effects and different imperfections. Visually, we can see different distinctive patterns with some similarities between modulations. It is not easy to visually discriminate between modulations based on the raw received signals by a human expert, particularly under noisy conditions.

Of course, we observe that the received signals are distorted, making the automatic recognition of one particular modulation by human eyes challenging. Thus, this study aims to develop a data-driven modulation identification approach by combining the power of the GAN model as a feature extractor and the sensitivity of the 1SVM in anomaly detection.

In this study, we concatenate the imaginary and real values of the received signals under different SNR levels for each modulation type. This enables augmenting the size of the data sets comparing of using amplitude or phase. Then, data is normalized, and for each class, 80% is used for training and 20% for testing. For the testing, 20% of the target class (inliers) is merged with the other classes (outliers) to evaluate the proposed approach's capability to distinguish between inliers and outliers. This procedure (testing) is repeated for all classes. This paper combines a generative deep learning model, namely GAN, as a features extractor and detector, namely 1SVM, to detect a given modulation class. Of course, we designed six GAN-1SVM-based modulation detectors based on features of only received signals of one type of modulation.

### *B. MODULATION IDENTIFICATION*

In this section, two experiments are conducted to show the benefit of the proposed modulation identification approach. DBN and RBM [56], [57], popular unsupervised generative models, were considered the reference methods for comparison. RBMs are generative stochastic models designed with a simple architecture constituted only by two layers. The Contrastive Divergence algorithm using Gibbs sampling is employed in RBM training, which is relatively slow [56]. On the other hand, DBN, which is constructed by stacking several RBMs, is trained to earn complex features via layer-by-layer learning strategy [57]. Unlike RBM and DBN, GAN does not use Monte Carlo approximation in training. For more details on DBN and RBM, see [58]. The first experiment

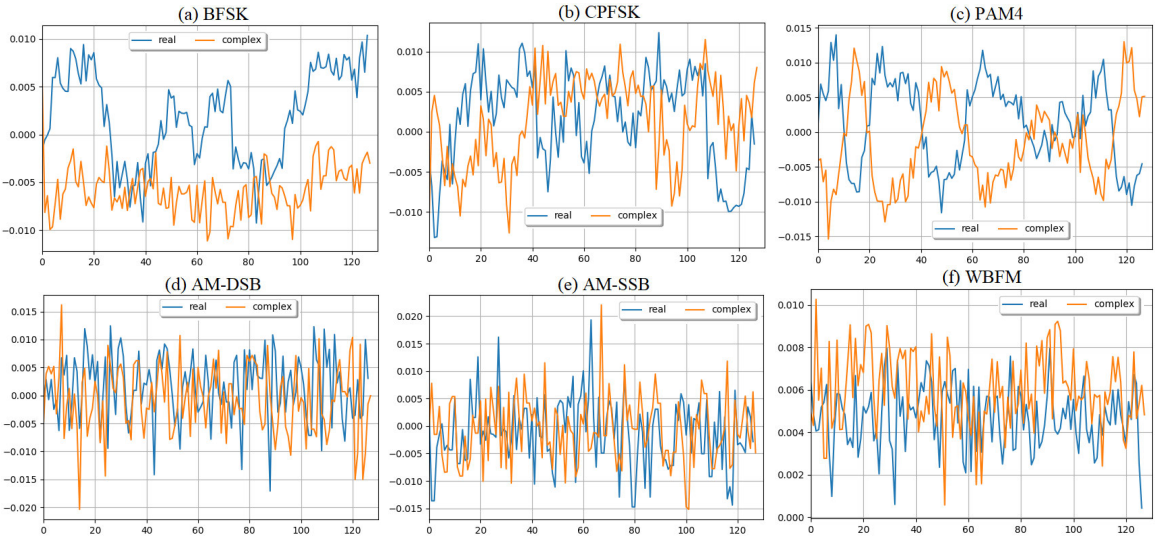


**FIGURE 7.** Example of received signals of different modulation types: (a) BFSK, (b) CPFSK, (c) PAM4, (d) AM-DSB, (e) AM-SSB, and (f) WB-FM.

assessed the performance of GAN, DBA, and RBM-based Softmax classifiers for modulation classification. A softmax classifier tops RBM and DBN for multiclass modulation classification. For GAN-based multiclass classification, a SoftMax classifier is placed at the output of the GAN discriminator. On the other hand, the second experiment aimed to verify the performance of the GAN, DBA, and RBM-based 1SVM detectors for modulation identification. The experiments in this study are conducted using an Intel i7 CPU, 12 Gigabytes for memory. The implemented approaches are performed using Python 3.6 with Tensorflow 2.3, Keras 2.2, and Scikit-learn 0.20 under Ubuntu 18.04 LTS.

At first, the models were trained based on training data. The values of the tuned parameters of the trained models are listed in Table 2. All the hyper-parameters are computed during the models training by the minimization of the cross-entropy of the reconstructed error.

**TABLE 2.** Tuned parameters in the investigated approaches.

| Model | Parameters |
|---|---|
| 1SVM | kernel=RBF kernel, nu=0.01, gamma=0.2 |
| RBM | layers: (visible layer 6, hidden layer 32), Dense(1, activation='Sigmoid'), Epochs=500, n_gibbs_steps = 5, Loss=Cross Entropy, Optimizer=Rmsprop |
| DBN | layers: 02 RBMs, Epochs=500, $batch_size = 1024, n\_hidden = (64, 32), n\_gibbs\_steps = 5, Optimizer = Rmsprop, Loss = CrossEntropy$ |
| GAN | Generator: 03 Layers (32, 64, 30), Discriminator: 03 Layers (30, 60, 32), Epochs=500, Batch size = 1024, Loss=Cross Entropy, Optimizer=Rmsprop |

In RBM, DBN, and GAN-based Softmax classifiers, the training data includes labeled data from all modulation types. This will help distinguish between them through computing the probability of belonging to a class using the softmax layer. A softmax classifier provides probabilities for each class. Indeed, the last layer is softmax in the investigated models (i.e., RBM, DBN, and GAN), acting as a classifier fed from a features space constructed by the deep models during the first phase of unsupervised training. The softmax layer is trained in a supervised manner permitting to fine-tune and adjust the deep model parameters learned during its unsupervised training. Specifically, the second stage of training is conducted in supervised learning (fine-tune), where the deep generative considered models parameters are adjusted and optimized to improve the classification performance.

Modulation classification results of RBM, DBN, and GAN-based Softmax classifiers using testing data are tabulated in Tables (3-5). We first observe that the GAN-based Softmax slightly outperformed RBM and DBN-based Softmax. Specifically, the GAN-based Softmax classifier reached an averaged accuracy and AUC of 0.56 and 0.54, respectively (Table 5). While RBM and DBN recorded an averaged AUC of 0.51 and 0.53, respectively, and an averaged accuracy of 0.53 and 0.54, respectively (Tables 3 and 4). The obtained results show the RBM, DBN, and GAN-based Softmax classifiers are not able to accurately discriminate the considered types of modulations. Even with the high capacity of the GAN-driven deep learning model in extracting relevant information from input signals, the GAN-based 1SVM classifier cannot accurately discriminate between the six considered modulations. These unsatisfactory classification results could be attributed to the limitation of the Softmax classifier in separating nonlinear features. Specifically, the Softmax classifier can only represent linear classification boundaries, which limits its discrimination ability. In addition, this unsuited result indicates that separating these different modulations is not an easy task.

**TABLE 3.** MC results using RBM-based softmax.

| Classes | Accuracy | Precision | Recall | F1-Score | AUC |
|---|---|---|---|---|---|
| AM-DSB | 0.68 | 0.50 | 0.68 | 0.57 | 0.54 |
| AM-SSB | 0.89 | 0.41 | 0.89 | 0.56 | 0.55 |
| CPFSK | 0.31 | 0.71 | 0.31 | 0.43 | 0.47 |
| BPSK | 0.55 | 0.71 | 0.55 | 0.62 | 0.61 |
| PAM4 | 0.55 | 0.71 | 0.55 | 0.62 | 0.61 |
| WBFM | 0.22 | 0.41 | 0.22 | 0.28 | 0.27 |

**TABLE 4.** MC results using DBN-based softmax.

| Classes | Accuracy | Precision | Recall | F1-Score | AUC |
|---|---|---|---|---|---|
| AM-DSB | 0.50 | 0.57 | 0.50 | 0.53 | 0.52 |
| AM-SSB | 0.69 | 0.45 | 0.69 | 0.54 | 0.53 |
| CPFSK | 0.50 | 0.47 | 0.50 | 0.49 | 0.48 |
| BPSK | 0.60 | 0.63 | 0.60 | 0.61 | 0.60 |
| PAM4 | 0.57 | 0.72 | 0.57 | 0.64 | 0.64 |
| WBFM | 0.38 | 0.51 | 0.38 | 0.43 | 0.43 |

**TABLE 5.** MC results using GAN-based softmax.

| Classes | Accuracy | Precision | Recall | F1-Score | AUC |
|---|---|---|---|---|---|
| AM-DSB | 0.72 | 0.50 | 0.72 | 0.59 | 0.57 |
| AM-SSB | 0.86 | 0.40 | 0.86 | 0.55 | 0.54 |
| CPFSK | 0.37 | 0.89 | 0.37 | 0.53 | 0.56 |
| BPSK | 0.62 | 0.59 | 0.62 | 0.61 | 0.60 |
| PAM4 | 0.63 | 0.96 | 0.63 | 0.76 | 0.75 |
| WBFM | 0.18 | 0.56 | 0.18 | 0.27 | 0.25 |

In the second experiment, the effectiveness of the unsupervised GAN, RBM, and DBN-based 1SVM detectors to discriminate the type of modulation in a MIMO system is investigated. Contrary to the previous experiment using supervised classification, we merge the features extraction ability of the RBM, DBN, and GAN models and the detection sensitivity of the 1SVM. In other words, we treat modulation identification as a multiple binary discrimination problem without considering labeled data. Modulation identification results when applying RBM, DBN, and GAN-based 1SVM detectors are listed in Tables 6, 7, and 8, respectively. Results in Tables (6-8) exhibit that the amalgamation of the deep learning models with the 1SVM detector considerably improved the capacity of modulation recognition compared to the previous results obtained with RBM, DBN, GAN-based Softmax classifier (Tables (3- 5)). The proposed GAN-based 1SVM detector offers superior discrimination performance of modulation types by achieving an averaged accuracy of 0.951 and F1-Score of 0.954. The DBN-based 1SVM obtained an averaged accuracy of 0.911 and an F1-Score of 0.913. The RBM-based 1SVM approach almost reached comparable detection performance to the DBN-1SVM approach with averaged accuracy of 0.912 and an F1-Score of 0.914.

To recapitulate the evaluations, we provide the barplot of the averaged AUC values per method in Figure 8 and as per method in Figure 9. Overall, Figure 8 confirms that the GAN-1SVM dominates the other models (RBM and DBN-based 1SVM) by showing better detection performance

**TABLE 6.** MC results using RBM-based 1SVM.

| Target | Classes | Accuracy | Precision | Recall | F1-score | AUC |
|---|---|---|---|---|---|---|
| AM-DSB | AM-SSB | 0.944 | 0.957 | 0.93 | 0.943 | 0.944 |
| AM-DSB | CPFSK | 0.956 | 0.963 | 0.948 | 0.956 | 0.956 |
| AM-DSB | BPSK | 0.964 | 0.975 | 0.952 | 0.964 | 0.964 |
| AM-DSB | PAM4 | 0.964 | 0.981 | 0.946 | 0.963 | 0.964 |
| AM-DSB | WBFM | 0.947 | 0.961 | 0.932 | 0.946 | 0.947 |
| AM-SSB | AM-DSB | 0.845 | 0.789 | 0.942 | 0.859 | 0.845 |
| AM-SSB | CPFSK | 0.855 | 0.811 | 0.926 | 0.865 | 0.855 |
| AM-SSB | BPSK | 0.852 | 0.794 | 0.95 | 0.865 | 0.852 |
| AM-SSB | PAM4 | 0.87 | 0.819 | 0.95 | 0.880 | 0.87 |
| AM-SSB | WBFM | 0.86 | 0.800 | 0.96 | 0.873 | 0.86 |
| CPFSK | AM-DSB | 0.887 | 0.849 | 0.942 | 0.893 | 0.887 |
| CPFSK | AM-SSB | 0.883 | 0.849 | 0.932 | 0.888 | 0.883 |
| CPFSK | BPSK | 0.885 | 0.840 | 0.952 | 0.892 | 0.885 |
| CPFSK | PAM4 | 0.884 | 0.854 | 0.926 | 0.889 | 0.884 |
| CPFSK | WBFM | 0.886 | 0.847 | 0.942 | 0.892 | 0.886 |
| BPSK | AM-DSB | 0.946 | 0.936 | 0.958 | 0.947 | 0.946 |
| BPSK | AM-SSB | 0.96 | 0.953 | 0.968 | 0.960 | 0.96 |
| BPSK | CPFSK | 0.944 | 0.934 | 0.956 | 0.945 | 0.944 |
| BPSK | PAM4 | 0.941 | 0.926 | 0.958 | 0.942 | 0.941 |
| BPSK | WBFM | 0.944 | 0.939 | 0.95 | 0.944 | 0.944 |
| PAM4 | AM-DSB | 0.874 | 0.883 | 0.862 | 0.872 | 0.874 |
| PAM4 | AM-SSB | 0.86 | 0.873 | 0.842 | 0.857 | 0.86 |
| PAM4 | CPFSK | 0.861 | 0.897 | 0.816 | 0.854 | 0.861 |
| PAM4 | BPSK | 0.856 | 0.872 | 0.834 | 0.853 | 0.856 |
| PAM4 | WBFM | 0.868 | 0.872 | 0.862 | 0.867 | 0.868 |
| WBFM | AM-DSB | 0.964 | 0.979 | 0.948 | 0.963 | 0.964 |
| WBFM | AM-SSB | 0.956 | 0.973 | 0.938 | 0.955 | 0.956 |
| WBFM | CPFSK | 0.966 | 0.981 | 0.95 | 0.965 | 0.966 |
| WBFM | BPSK | 0.962 | 0.981 | 0.942 | 0.961 | 0.962 |
| WBFM | PAM4 | 0.966 | 0.979 | 0.952 | 0.966 | 0.966 |

**TABLE 7.** MC results using DBN-based 1SVM.

| Target | Classes | Accuracy | Precision | Recall | F1-score | AUC |
|---|---|---|---|---|---|---|
| AM-DSB | AM-SSB | 0.95 | 0.957 | 0.942 | 0.950 | 0.95 |
| AM-DSB | CPFSK | 0.951 | 0.965 | 0.936 | 0.950 | 0.951 |
| AM-DSB | BPSK | 0.955 | 0.961 | 0.948 | 0.955 | 0.955 |
| AM-DSB | PAM4 | 0.949 | 0.959 | 0.938 | 0.948 | 0.949 |
| AM-DSB | WBFM | 0.96 | 0.962 | 0.958 | 0.960 | 0.96 |
| AM-SSB | AM-DSB | 0.838 | 0.780 | 0.942 | 0.853 | 0.838 |
| AM-SSB | CPFSK | 0.852 | 0.792 | 0.954 | 0.866 | 0.852 |
| AM-SSB | BPSK | 0.856 | 0.803 | 0.944 | 0.868 | 0.856 |
| AM-SSB | PAM4 | 0.853 | 0.795 | 0.952 | 0.866 | 0.853 |
| AM-SSB | WBFM | 0.858 | 0.792 | 0.972 | 0.873 | 0.858 |
| CPFSK | AM-DSB | 0.888 | 0.845 | 0.95 | 0.895 | 0.888 |
| CPFSK | AM-SSB | 0.895 | 0.848 | 0.962 | 0.902 | 0.895 |
| CPFSK | BPSK | 0.895 | 0.852 | 0.956 | 0.901 | 0.895 |
| CPFSK | PAM4 | 0.878 | 0.835 | 0.942 | 0.885 | 0.878 |
| CPFSK | WBFM | 0.872 | 0.826 | 0.942 | 0.880 | 0.872 |
| BPSK | AM-DSB | 0.963 | 0.958 | 0.968 | 0.963 | 0.963 |
| BPSK | AM-SSB | 0.949 | 0.946 | 0.952 | 0.949 | 0.949 |
| BPSK | CPFSK | 0.939 | 0.931 | 0.948 | 0.940 | 0.939 |
| BPSK | PAM4 | 0.943 | 0.942 | 0.944 | 0.943 | 0.943 |
| BPSK | WBFM | 0.939 | 0.930 | 0.95 | 0.940 | 0.939 |
| PAM4 | AM-DSB | 0.865 | 0.889 | 0.834 | 0.861 | 0.865 |
| PAM4 | AM-SSB | 0.858 | 0.891 | 0.816 | 0.852 | 0.858 |
| PAM4 | CPFSK | 0.863 | 0.889 | 0.83 | 0.858 | 0.863 |
| PAM4 | BPSK | 0.88 | 0.906 | 0.848 | 0.876 | 0.88 |
| PAM4 | WBFM | 0.871 | 0.904 | 0.83 | 0.865 | 0.871 |
| WBFM | AM-DSB | 0.972 | 0.974 | 0.97 | 0.972 | 0.972 |
| WBFM | AM-SSB | 0.959 | 0.973 | 0.944 | 0.958 | 0.959 |
| WBFM | CPFSK | 0.96 | 0.981 | 0.938 | 0.959 | 0.96 |
| WBFM | BPSK | 0.959 | 0.966 | 0.952 | 0.959 | 0.959 |
| WBFM | PAM4 | 0.956 | 0.962 | 0.95 | 0.956 | 0.956 |

in identifying modulation types from the received signals. In addition, both digital and analog modulation can be recognized by the proposed GAN-1SVM approach.

In summary, these results prove that the GAN-1SVM approach provided satisfactory results in identifying modulation types from the received signals. The main reason that the proposed hybrid approach outperformed the rest of the methods is related to its principle-based on (i) the recognition

**TABLE 8.** MC results using GAN-based 1SVM.

| Target | Classes | Accuracy | Precision | Recall | F1-Score | AUC |
|---|---|---|---|---|---|---|
| AM-DSB | AM-SSB | 0.976 | 1 | 0.952 | 0.975 | 0.976 |
| AM-DSB | CPFSK | 0.972 | 1 | 0.944 | 0.971 | 0.972 |
| AM-DSB | BPSK | 0.959 | 0.973 | 0.944 | 0.958 | 0.959 |
| AM-DSB | PAM4 | 0.977 | 0.998 | 0.956 | 0.977 | 0.977 |
| AM-DSB | WBFM | 0.954 | 0.971 | 0.936 | 0.953 | 0.954 |
| AM-SSB | AM-DSB | 0.967 | 0.974 | 0.96 | 0.967 | 0.967 |
| AM-SSB | CPFSK | 0.959 | 0.966 | 0.952 | 0.959 | 0.959 |
| AM-SSB | BPSK | 0.962 | 0.977 | 0.946 | 0.961 | 0.962 |
| AM-SSB | PAM4 | 0.955 | 0.952 | 0.958 | 0.955 | 0.955 |
| AM-SSB | WBFM | 0.969 | 0.976 | 0.962 | 0.969 | 0.969 |
| CPFSK | AM-DSB | 0.767 | 0.697 | 0.944 | 0.802 | 0.767 |
| CPFSK | AM-SSB | 0.972 | 1 | 0.944 | 0.971 | 0.972 |
| CPFSK | BPSK | 0.853 | 0.791 | 0.96 | 0.867 | 0.853 |
| CPFSK | PAM4 | 0.917 | 0.899 | 0.94 | 0.919 | 0.917 |
| CPFSK | WBFM | 0.78 | 0.706 | 0.96 | 0.814 | 0.78 |
| BPSK | AM-DSB | 0.978 | 0.998 | 0.958 | 0.978 | 0.978 |
| BPSK | AM-SSB | 0.973 | 1 | 0.946 | 0.972 | 0.973 |
| BPSK | CPFSK | 0.971 | 0.994 | 0.948 | 0.970 | 0.971 |
| BPSK | PAM4 | 0.978 | 1 | 0.956 | 0.978 | 0.978 |
| BPSK | WBFM | 0.967 | 0.978 | 0.956 | 0.967 | 0.967 |
| PAM4 | AM-DSB | 0.974 | 1 | 0.948 | 0.973 | 0.974 |
| PAM4 | AM-SSB | 0.981 | 1 | 0.962 | 0.981 | 0.981 |
| PAM4 | CPFSK | 0.988 | 1 | 0.976 | 0.988 | 0.988 |
| PAM4 | BPSK | 0.975 | 1 | 0.95 | 0.974 | 0.975 |
| PAM4 | WBFM | 0.977 | 1 | 0.954 | 0.976 | 0.977 |
| WBFM | AM-DSB | 0.938 | 0.942 | 0.934 | 0.938 | 0.938 |
| WBFM | AM-SSB | 0.972 | 1 | 0.944 | 0.971 | 0.972 |
| WBFM | CPFSK | 0.984 | 1 | 0.968 | 0.984 | 0.984 |
| WBFM | BPSK | 0.972 | 0.996 | 0.948 | 0.971 | 0.972 |
| WBFM | PAM4 | 0.968 | 1 | 0.936 | 0.967 | 0.968 |

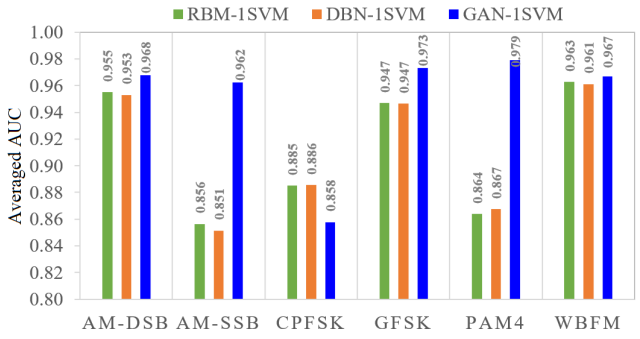


**FIGURE 8.** Averaged AUC values per modulation.

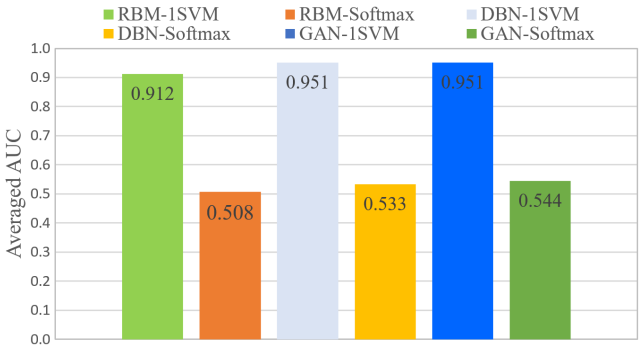


**FIGURE 9.** Averaged AUC values by method.

of each class separately, (ii) the approximation of the data distribution by the creation of latent space, which is appropriate in the representation of original data, and (iii) the high capability of 1SVM in separating atypical features from the training data.

Now, the execution time of the considered models is analyzed. We conducted all experiments using CPU intel i3 with 8 G.B to guarantee a fair comparison. We implemented the investigated methods via Python with Tensorflow 2.3, Keras, and Scikit-Learn 0.22. The averaged testing times of the GAN-1SVM, DBN-1SVM, and RBM-1SVM are 0.3057, 0.24, and 0.21, respectively. We observe that the RBM-1SVM approach requires a lower testing time compared to DBN-1SVM and GAN-1SVM. The RBM model has a simple structure compared to DBN and GAN models. The GAN-1SVM model requires, on average, 0.3057s for testing, in which the average of 1SVM predicting time is 0.000325s. Note that the training is performed offline, and once the model is trained, it can be used for detection. After training the GAN model, we used only the discriminator model, a feed-forward neural network. Each hidden neuron performs a linear combination of inputs $X$ and applies a non-linear (or activation) function: sigmoid ($XW$ + b) with W and $b$ are respectively the weights matrix and bias vector. It is worth noting that the central characteristic of a model is its capability to accurately recognize the modulation type. Thus, there exists a trade-off between training time and performance. The RBM-1SVM and DBN-1SVM approaches require less training time, but the GAN-1SVN shows better detection performance. In addition, the training is performed offline. Crucially, the selection of the modulation identification approach should be based not only on detection accuracy but also on model complexity. The time complexity provides relevant information about the time needed for the investigated model for the execution, generally computed using $O$ notation. Assume that an algorithm will process $n$ data points. An algorithm will have a constant complexity (i.e., $O(1)$) if not relying on $n$. However, if the model depends on $n$, the complexity depends on the line code in the model (e.g., $O(n)$, $O(n^2)$) [59].

The computational complexity of deep learning models (e.g., GAN, DBN, and RBM) relies principally on the structure of the model: the number of layers and the number of neurons in each layer. The time complexity of the proposed GAN-1SVM approach can be evaluated with regard to feature extraction by the GAN model and modulation identification using the 1SVM algorithm. The primary components of the GAN architecture are two neural networks: an encoder and a decoder. As described in TAble 2, the GAN encoder and decoder consist of a neural network with three layers. The time complexity of neural networks during training and testing are $O(dNtrIL)$ and $O(dNte)$, respectively [60]. Where $d$ is the data dimension, $L$ denotes the number of layers, $Ntr$ is the number of training data points, $Nte$ denotes the number of testing data points. The time complexity of 1SVM is $O(Nte^3)$ [59], [61]. Then, the total computational complexity of the GAN-1SVM model in training is $O(2(dNtrIL) + (Nte^3))$. As reported in [62], the time complexity of DBN is similar to that of SVM, $O(Nte^3)$, which is relatively high. The time complexity for training the RBM model is $O(c(m + n))$,

where $n$ and $m$ denote the number of visible and hidden units, and $c$ denotes the number of iterations [57], [63].

### C. COMPARISON WITH THE STATE-OF-THE-ART

This section compares the performance of the proposed RBM, DBN, and GAN-based 1SVM detectors with state-of-the-art (SOTA) methods applied to RadioML 2016.10a. Several deep learning-driven methods have been developed to address the problem of automatic modulation recognition, including LSTM [64], CNN [65], CNN-LSTM [66], CLDNN [65], CM-CNN [65], SCNN2 [67], combined Fourth-order cumulant with SVM [68], 2-layer GAM-HRNN-GRU [69], and GAM-HRNN-GRU [69]. Table 9 compares the achieved average accuracy of the proposed approaches (RBM, DBN, and GAN-based 1SVM) with those of the state-of-the-art methods. It should be noted that the average accuracies of the SOTA methods listed in Table 9 are estimated from the provided accuracy curves in the original papers. This is because the original papers do not provide specific classification accuracy values. Table 9 shows that combining traditional feature extractors with shallow classifiers leads to the worst recognition performance. Specifically, in [68], an approach combining higher-order cumulants and SVM for modulation classification. Specifically, high-order cumulants are extracted from the received signals and used as input for the SVM to classify modulation types. This combined approach achieved improved performance than the standalone SVM, but its average classification accuracy is not satisfactory, i.e., 0.473. This indicates that traditional features are not efficient in characterizing the modulation schemes of received signals, maybe due to the different effects of various noises. The study in [65] introduced a correction module (CM) to mitigate signal distortion to improve the modulation accuracy. They revealed that CM combined with CNN, CM+CNN, achieved better accuracy (0.59) than CNN (0.52) and Convolutional Long short-term Deep Neural Networks (CLDNN) (0.55). However, the classification accuracy is still below the desired performance even with CM. Authors in [67] presented a spectrum analysis-based convolutional neural network (SCNN) scheme for modulation classification and achieved an accuracy of 0.611. This approach applies SCNN to spectrogram images obtained by applying the short-time discrete Fourier transform to the observed signals. In [70], an approach called LSTM-IQFOC achieved an average accuracy of 0.519 by merging the raw In-Phase and Quadrature (IQ) data, Fourth-order Cumulants (FOC), and LSTM for modulation recognition. Besides, the average accuracy obtained by using LSTM [70] is 0.624. This means that the modulation recognition has not been improved even by using powerful deep learning models. In [69], by combining modified hierarchical recurrent neural networks with a grouped auxiliary memory GRU (GAM-HRNN-GRU), significantly improved results have been obtained by reaching an accuracy of 0.916. Also, in [69], an accuracy of 0.922 has been obtained by using the 2-layer GAM-HRNN-GRU approach. Table 9 revealed that the GAN-based 1SVM method outperformed the SOTA methods by achieving a satisfying recognition accuracy of 0.951. Thus, we can deduce that the GAN-1SVM scheme is well adapted for discriminating modulation schemes from the received signals and presents an effective and flexible way for automatic modulation recognition than other deep learning-driven methods.

**TABLE 9. Comparison with the state-of-the-art methods.**

| Refs | Model | Average accuracy |
|---|---|---|
| [67] | SCNN2 | 0.611 |
| [68] | Fourth-order cumulant + SVM | 0.473 |
| [69] | 2-layer GAM-HRNN-GRU | 0.922 |
| [69] | GAM-HRNN-GRU | 0.916 |
| [64] | LSTM | 0.624 |
| [70] | LSTM-IQFOC | 0.519 |
| [65] | CNN | 0.520 |
| [65] | CLDNN | 0.550 |
| [65] | CM-CNN | 0.590 |
| **Proposed** | **RBM-1SVM** | **0.912** |
| **Proposed** | **DBN-1SVM** | **0.911** |
| **Proposed** | **GAN-1SVM** | **0.951** |

## VI. CONCLUSION

To guarantee reliable performances complying with wireless communication, accurate recognition of modulation types of signals is becoming an indispensable component in MIMO systems. This study introduced a semi-supervised deep learning-based strategy for modulation discrimination in MIMO systems. Importantly, we addressed the problem of multiclass classification as an anomaly detection problem based on unlabeled data. The designed data-based scheme merges the extended capacity of the GAN features extractor and the discrimination ability of the 1SVM-based anomaly detection scheme. Specifically, the 1SVM detector is applied to the features extracted by the GAN model for separating modulation types. The efficiency of the proposed method is verified using the public datasets RadioML.2016.10a. Five statistical scores have been utilized to judge the detection accuracy of the studied methods, including accuracy, precision, recall, F1-Score, and AUC. Results revealed that the proposed GAN-1SVM offers superior discrimination performance of modulation types and dominates the investigated methods (RBM and DBN-based 1SVM) and the state-of-the-art techniques.

Despite the improved identification of the modulation type from the received signal using the GAN-1SVM, future works will be aimed at improving the robustness of the GAN-1SVM model to noisy measurements by developing a wavelet-based GAN-1SVM detector. To this end, we will use wavelet decomposition to capture multivariate information in the time and frequency domains and then employ a GAN model to extract relevant features that will be fed to the 1SVM for modulation identification. It is expected that by applying wavelet-based multiscale denoising to the received signals, noise effects will be reduced, thus improving

the modulation recognition of the GAN-1SVM. Furthermore, another direction of improvement consists of using data augmentation techniques to generate large-sized data, which improves the construction of deep learning models and thus enhances modulation recognition. Although the proposed GAN-1SVM approach provided superior performance for automatic modulation recognition than the other models, this approach has a significant execution time cost. An interesting direction for future work is to further reduce its computational complexity while maintaining high modulation recognition accuracy. This could be done by integrating feature selection procedures or incorporating an attention mechanism in the GAN model to focus only on the relevant features.

## REFERENCES

[1] S. Bouchenak, R. Merzougui, and F. Harrou, "A hybrid beamforming massive MIMO system for 5G: Performance assessment study," in *Proc. Int. Conf. Innov. Intell. Informat., Comput., Technol. (ICT)*, Sep. 2021, pp. 371–375.

[2] M. R. Bahloul, M. Z. Yusoff, A.-H. Abdel-Aty, M. N. M. Saad, and M. Al-Jemeli, "Modulation classification for MIMO systems: State of the art and research directions," *Chaos, Solitons Fractals*, vol. 89, pp. 497–505, Aug. 2016.

[3] Q. Zheng, P. Zhao, Y. Li, H. Wang, and Y. Yang, "Spectrum interference-based two-level data augmentation method in deep learning for automatic modulation classification," *Neural Comput. Appl.*, vol. 33, no. 13, pp. 7723–7745, Nov. 2020.

[4] B. Ramkumar, "Automatic modulation classification for cognitive radios using cyclic feature detection," *IEEE Circuits Syst. Mag.*, vol. 9, no. 2, pp. 27–45, Jun. 2009.

[5] Y. A. Eldemerdash, O. A. Dobre, O. Üreten, and T. Yensen, "A robust modulation classification method for PSK signals using random graphs," *IEEE Trans. Instrum. Meas.*, vol. 68, no. 2, pp. 642–644, Feb. 2018.

[6] R. A. Poisel, *Introduction to Communication Electronic Warfare Systems*. Norwood, MA, USA: Artech House, 2002.

[7] Z. Zhu and A. K. Nandi, *Automatic Modulation Classification: Principles, Algorithms and Applications*. Hoboken, NJ, USA: Wiley 2015.

[8] M. Narendar, A. P. Vinod, A. S. M. Kumar, and A. K. Krishna, "Automatic modulation classification for cognitive radios using cumulants based on fractional lower order statistics," in *Proc. 30th URSI Gen. Assem. Sci. Symp.*, Aug. 2011, pp. 1–4.

[9] O. A. Dobre, "Signal identification for emerging intelligent radios: Classical problems and new challenges," *IEEE Instrum. Meas. Mag.*, vol. 18, no. 2, pp. 11–18, Apr. 2015.

[10] H. B. Chikha, A. Almadhor, and W. Khalid, "Machine learning for 5G MIMO modulation detection," *Sensors*, vol. 21, no. 5, p. 1556, Feb. 2021.

[11] M. S. Mühlhaus, M. Öner, O. A. Dobre, H. U. Jkel, and F. K. Jondral, "Automatic modulation classification for MIMO systems using fourth-order cumulants," in *Proc. IEEE Veh. Technol. Conf. (VTC Fall)*, Sep. 2012, pp. 1–5.

[12] E. Kanterakis and W. Su, "Modulation classification in MIMO systems," in *Proc. IEEE Mil. Commun. Conf.*, Nov. 2013, pp. 35–39.

[13] Z. Zhu and A. K. Nandi, "Blind modulation classification for MIMO systems using expectation maximization," in *Proc. IEEE Mil. Commun. Conf.*, Oct. 2014, pp. 754–759.

[14] J. Tian, Y. Pei, Y. D. Huang, and Y.-C. Liang, "Modulation-constrained clustering approach to blind modulation classification for MIMO systems," *IEEE Trans. Cogn. Commun. Netw.*, vol. 4, no. 4, pp. 894–907, Dec. 2018.

[15] Z. Xing and Y. Gao, "A modulation classification algorithm for multipath signals based on cepstrum," *IEEE Trans. Instrum. Meas.*, vol. 69, no. 7, pp. 4742–4752, Jul. 2020.

[16] H. Agirman-Tosun, Y. Liu, A. M. Haimovich, O. Simeone, W. Su, J. Dabin, and E. Kanterakis, "Modulation classification of MIMO-OFDM signals by independent component analysis and support vector machines," in *Proc. Conf. Rec. 45th Asilomar Conf. Signals, Syst. Comput. (ASILOMAR)*, Nov. 2011, pp. 1903–1907.

[17] R. Utrilla, E. Fonseca, A. Araujo, and L. A. Dasilva, "Gated recurrent unit neural networks for automatic modulation classification with resource-constrained end-devices," *IEEE Access*, vol. 8, pp. 112783–112794, 2020.

[18] S. Peng, H. Jiang, H. Wang, H. Alwageed, Y. Zhou, M. M. Sebdani, and Y.-D. Yao, "Modulation classification based on signal constellation diagrams and deep learning," *IEEE Trans. Neural Netw. Learn. Syst.*, vol. 30, no. 3, pp. 718–727, Mar. 2018.

[19] Z. Zhang, H. Luo, C. Wang, C. Gan, and Y. Xiang, "Automatic modulation classification using CNN-LSTM based dual-stream structure," *IEEE Trans. Veh. Technol.*, vol. 69, no. 11, pp. 13521–13531, Oct. 2020.

[20] F. Harrou, Y. Sun, A. S. Hering, and M. Madakyaru, *Statistical Process Monitoring Using Advanced Data-Driven and Deep Learning Approaches: Theory and Practical Applications*. Amsterdam, The Netherlands: Elsevier, 2020.

[21] B. Mao, F. Tang, Z. M. Fadlullah, and N. Kato, "An intelligent route computation approach based on real-time deep learning strategy for software defined communication systems," *IEEE Trans. Emerg. Topics Comput.*, vol. 9, no. 3, pp. 1554–1565, Jul. 2021.

[22] H. Huang, S. Guo, G. Gui, Z. Yang, J. Zhang, H. Sari, and F. Adachi, "Deep learning for physical-layer 5G wireless techniques: Opportunities, challenges and solutions," *IEEE Wireless Commun.*, vol. 27, no. 1, pp. 214–222, Feb. 2019.

[23] H. Huang, Y. Peng, J. Yang, W. Xia, and G. Gui, "Fast beamforming design via deep learning," *IEEE Trans. Veh. Technol.*, vol. 69, no. 1, pp. 1065–1069, Jan. 2019.

[24] J. Huang, S. Huang, Y. Zeng, H. Chen, S. Chang, and Y. Zhang, "Hierarchical digital modulation classification using cascaded convolutional neural network," *J. Commun. Inf. Netw.*, vol. 6, no. 1, pp. 72–81, Mar. 2021.

[25] B. Kim, J. Kim, H. Chae, D. Yoon, and J. W. Choi, "Deep neural network-based automatic modulation classification technique," in *Proc. Int. Conf. Inf. Commun. Technol. Converg. (ICTC)*, Oct. 2016, pp. 579–582.

[26] X. Liu, D. Yang, and A. E. Gamal, "Deep neural network architectures for modulation classification," in *Proc. 51st Asilomar Conf. Signals, Syst., Comput.*, Oct. 2017, pp. 915–919.

[27] M. R. Bahloul, M. Z. Yusoff, A.-H. Abdel-Aty, M. N. Saad, and A. Laouiti, "Efficient and reliable modulation classification for MIMO systems," *Arabian J. Sci. Eng.*, vol. 42, no. 12, pp. 5201–5209, Dec. 2017.

[28] M. Sarfraz, S. Alam, S. A. Ghauri, A. Mahmood, M. N. Akram, M. J. U. Rehman, M. F. Sohail, and T. M. Kebedew, "Random graph-based M-QAM classification for MIMO systems," *Wireless Commun. Mobile Comput.*, vol. 2022, pp. 1–10, Apr. 2022.

[29] T. Huynh-The, T.-V. Nguyen, Q.-V. Pham, D. B. da Costa, and D.-S. Kim, "MIMO-OFDM modulation classification using three-dimensional convolutional network," *IEEE Trans. Veh. Technol.*, vol. 71, no. 6, pp. 6738–6743, Jun. 2022.

[30] Y. Wang, J. Gui, Y. Yin, J. Wang, J. Sun, G. Gui, H. Gacanin, H. Sari, and F. Adachi, "Automatic modulation classification for MIMO systems via deep learning and zero-forcing equalization," *IEEE Trans. Veh. Technol.*, vol. 69, no. 5, pp. 5688–5692, May 2020.

[31] H. Ben Chikha and A. Almadhor, "Automatic classification of superimposed modulations for 5G MIMO two-way cognitive relay networks," *Comput., Mater. Continua*, vol. 70, no. 1, pp. 1799–1814, 2022.

[32] Z. Gao, Z. Zhu, and A. K. Nandi, "Modulation classification in MIMO systems with distribution test ensemble," *IEEE Access*, vol. 8, pp. 128819–128829, 2020.

[33] Y. Wang, J. Wang, W. Zhang, J. Yang, and G. Gui, "Deep learning-based cooperative automatic modulation classification method for MIMO systems," *IEEE Trans. Veh. Technol.*, vol. 69, no. 4, pp. 4575–4579, Apr. 2020.

[34] T. Zhang, C. Shuai, and Y. Zhou, "Deep learning for robust automatic modulation recognition method for IoT applications," *IEEE Access*, vol. 8, pp. 117689–117697, 2020.

[35] Y. A. Eldemerdash, O. A. Dobre, and M. Öner, "Signal identification for multiple-antenna wireless systems: Achievements and challenges," *IEEE Commun. Surveys Tuts.*, vol. 18, no. 3, pp. 1524–1551, 3rd Quart., 2016.

[36] O. A. Dobre, A. Abdi, Y. Bar-Ness, and W. Su, "Survey of automatic modulation classification techniques: Classical approaches and new trends," *IET Commun.*, vol. 1, no. 2, pp. 137–156, Apr. 2007.

[37] S. Peng, S. Sun, and Y.-D. Yao, "A survey of modulation classification using deep learning: Signal representation and data preprocessing," *IEEE Trans. Neural Netw. Learn. Syst.*, early access, Jun. 14, 2021, doi: 10.1109/TNNLS.2021.3085433.

[38] X. Yang, "An ensemble automatic modulation classification model with weight pruning and data preprocessing," Ph.D. dissertation, Dept. Elect. Comput. Eng., Univ. British Columbia, Vancouver, BC, Canada, 2020.

[39] M. Kulin, T. Kazaz, I. Moerman, and E. De Poorter, "End-to-end learning from spectrum data: A deep learning approach for wireless signal identification in spectrum monitoring applications," *IEEE Access*, vol. 6, pp. 18484–18501, 2018.
[40] A. Creswell, T. White, V. Dumoulin, K. Arulkumaran, B. Sengupta, and A. A. Bharath, "Generative adversarial networks: An overview," *IEEE Signal Process.*, vol. 35, no. 1, pp. 53–65, Jan. 2018.
[41] L. Zhu, Y. Chen, P. Ghamisi, and J. A. Benediktsson, "Generative adversarial networks for hyperspectral image classification," *IEEE Trans. Geosci. Remote Sens.*, vol. 56, no. 9, pp. 5046–5063, Sep. 2018.
[42] I. Goodfellow, J. Pouget-Abadie, M. Mirza, B. Xu, D. Warde-Farley, S. Ozair, A. Courville, and Y. Bengio, "Generative adversarial networks," *Commun. ACM*, vol. 63, no. 11, pp. 139–144, 2020.
[43] F. Kadri, A. Dairi, F. Harrou, and Y. Sun, "Towards accurate prediction of patient length of stay at emergency department: A GAN-driven deep learning framework," *J. Ambient Intell. Humanized Comput.*, pp. 1–15, Feb. 2022, doi: 10.1007/s12652-022-03717-z.
[44] W. Fedus, M. Rosca, B. Lakshminarayanan, A. M. Dai, S. Mohamed, and I. Goodfellow, "Many paths to equilibrium: GANs do not need to decrease a divergence at every step," 2017, *arXiv:1710.08446*.
[45] I. Goodfellow, J. Pouget-Abadie, M. Mirza, B. Xu, D. Warde-Farley, S. Ozair, A. Courville, and Y. Bengio, "Generative adversarial nets," in *Proc. Adv. Neural Inf. Process. Syst.*, vol. 27, 2014, pp. 1–9.
[46] H. J. Shin, D.-H. Eom, and S.-S. Kim, "One-class support vector machines—An application in machine fault detection and classification," *Comput. Ind. Eng.*, vol. 48, no. 2, pp. 395–408, Mar. 2005.
[47] F. Harrou, Y. Sun, A. S. Hering, M. Madakyaru, and A. Dairi, "Unsupervised deep learning-based process monitoring methods," in *Statistical Process Monitoring Using Advanced Data-Driven and Deep Learning Approaches*. Amsterdam, The Netherlands: Elsevier, 2021, pp. 193–223.
[48] F. Harrou, N. Zerrouki, A. Dairi, Y. Sun, and A. Houacine, "Automatic human fall detection using multiple tri-axial accelerometers," in *Proc. Int. Conf. Innov. Intell. Informat., Comput., Technol. (ICT)*, Sep. 2021, pp. 74–78.
[49] B. Schölkopf, J. C. Platt, J. C. Shawe-Taylor, A. J. Smola, and R. C. Williamson, "Estimating the support of a high-dimensional distribution," *Neural Comput.*, vol. 13, no. 7, pp. 1443–1471, 2001.
[50] F. Harrou, A. Dairi, B. Taghezouit, and Y. Sun, "An unsupervised monitoring procedure for detecting anomalies in photovoltaic systems using a one-class support vector machine," *Sol. Energy*, vol. 179, pp. 48–58, Feb. 2019.
[51] A. Dairi, F. Harrou, M. Senouci, and Y. Sun, "Unsupervised obstacle detection in driving environments using deep-learning-based stereovision," *Robot. Auto. Syst.*, vol. 100, pp. 287–301, Feb. 2018.
[52] F. Harrou, A. Dairi, Y. Sun, and F. Kadri, "Detecting abnormal ozone measurements with a deep learning-based strategy," *IEEE Sensors J.*, vol. 18, no. 17, pp. 7222–7232, Sep. 2018.
[53] T. Cheng, A. Dairi, F. Harrou, Y. Sun, and T. Leiknes, "Monitoring influent conditions of wastewater treatment plants by nonlinear data-based techniques," *IEEE Access*, vol. 7, pp. 108827–108837, 2019.
[54] T. J. O'Shea, J. Corgan, and T. C. Clancy, "Convolutional radio modulation recognition networks," in *Proc. Int. Conf. Eng. Appl. Neural Netw.* Cham, Switzerland: Springer, 2016, pp. 213–226.
[55] T. J. O'shea and N. West, "Radio machine learning dataset generation with gnu radio," in *Proc. GNU Radio Conf.*, vol. 1, 2016, pp. 1–6.
[56] G. E. Hinton, "A practical guide to training restricted Boltzmann machines," in *Neural Networks: Tricks of the Trade*. Cham, Switzerland: Springer, 2012, pp. 599–619.
[57] G. Hinton, S. Osindero, and Y.-W. Teh, "A fast learning algorithm for deep belief nets," *Neural Comput.*, vol. 18, no. 7, pp. 1527–1554, 1960.
[58] B. Ghojogh, A. Ghodsi, F. Karray, and M. Crowley, "Restricted Boltzmann machine and deep belief network: Tutorial and survey," 2021, *arXiv:2107.12521*.
[59] A. Abdiansah and R. Wardoyo, "Time complexity analysis of support vector machines (SVM) in LibSVM," *Int. J. Comput. Appl.*, vol. 128, no. 3, pp. 28–34, Oct. 2015.
[60] M. Z. Asghar, M. Abbas, K. Zeeshan, P. Kotilainen, and T. Hämäläinen, "Assessment of deep learning methodology for self-organizing 5G networks," *Appl. Sci.*, vol. 9, no. 15, p. 2975, Jul. 2019.
[61] R. Maji, A. Biswas, and R. Chaki, "A novel proposal of using NLP to analyze IoT apps towards securing user data," in *Proc. Int. Conf. Comput. Inf. Syst. Ind. Manage.* Cham, Switzerland: Springer, 2021, pp. 156–168.
[62] N. Burlutskiy, M. Petridis, A. Fish, A. Chernov, and N. Ali, "An investigation on online versus batch learning in predicting user behaviour," in *Proc. Int. Conf. Innov. Techn. Appl. Artif. Intell.* Cham, Switzerland: Springer, 2016, pp. 135–149.
[63] M. Sun, T. Min, T. Zang, and Y. Wang, "CDL4CDRP: A collaborative deep learning approach for clinical decision and risk prediction," *Processes*, vol. 7, no. 5, p. 265, May 2019.
[64] Y. Sang and L. Li, "Application of novel architectures for modulation recognition," in *Proc. IEEE Asia Pacific Conf. Circuits Syst. (APCCAS)*, Oct. 2018, pp. 159–162.
[65] K. Yashashwi, A. Sethi, and P. Chaporkar, "A learnable distortion correction module for modulation recognition," *IEEE Wireless Commun. Lett.*, vol. 8, no. 1, pp. 77–80, Feb. 2019.
[66] Y. Wu, X. Li, and J. Fang, "A deep learning approach for modulation recognition via exploiting temporal correlations," in *Proc. IEEE 19th Int. Workshop Signal Process. Adv. Wireless Commun. (SPAWC)*, Jun. 2018, pp. 1–5.
[67] Y. Zeng, M. Zhang, F. Han, Y. Gong, and J. Zhang, "Spectrum analysis and convolutional neural network for automatic modulation recognition," *IEEE Wireless Commun. Lett.*, vol. 8, no. 3, pp. 929–932, Jun. 2019.
[68] F. Yang, Z. Li, S. Zeng, B. Hao, P. Qi, and Z. Pang, "A novel method for wireless communication signal modulation recognition in smart grid," *J. Commun.*, vol. 11, no. 9, pp. 813–818, 2016.
[69] K. Zang and Z. Ma, "Automatic modulation classification based on hierarchical recurrent neural networks with grouped auxiliary memory," *IEEE Access*, vol. 8, pp. 213052–213061, 2020.
[70] M. Zhang, Y. Zeng, Z. Han, and Y. Gong, "Automatic modulation recognition using deep learning architectures," in *Proc. IEEE 19th Int. Workshop Signal Process. Adv. Wireless Commun. (SPAWC)*, Jun. 2018, pp. 1–5.